American Mineralogist, Volume 81, pages 341–348, 1996

Volume behavior of hydrous minerals at high pressure and temperature: II. Compressibilities of lawsonite, zoisite, clinozoisite, and epidote

T.J.B. HOLLAND,[1] S.A.T. REDFERN,[1] AND A.R. PAWLEY[2,*]

[1]Department of Earth Sciences, University of Cambridge, Downing Street, Cambridge CB2 3EQ, U.K.
[2]Department of Geology, University of Bristol, Wills Memorial Building, Queens Road, Bristol BS8 1RJ, U.K.

ABSTRACT

The pressure dependence of the lattice parameters of natural zoisite [$Ca_2Al_3Si_3O_{12}(OH)$], clinozoisite [$Ca_2Al_3Si_3O_{12}(OH)$], and epidote [$Ca_2Al_2FeSi_3O_{12}(OH)$] as well as synthetic lawsonite [$CaAl_2Si_2O_7(OH)_2 \cdot H_2O$] have been measured at ambient temperatures by energy-dispersive X-ray diffraction in a diamond-anvil cell. The experimental results for each phase may be summarized concisely in terms of the ambient-temperature isothermal bulk modulus K_{298} (using the Murnaghan equation of state and assuming $K' = 4$): Lawsonite: $K_{298} = 191 \pm 5$ GPa; zoisite: $K_{298} = 279 \pm 9$ GPa; clinozoisite: $K_{298} = 154 \pm 6$ GPa; epidote: $K_{298} = 162 \pm 4$ GPa. These new measurements, together with the new thermal expansion data in the companion paper (Pawley et al. 1996), were used to calculate some phase equilibria for lawsonite dehydration to high pressures for comparison with experimental brackets. Important discrepancies between calculated and experimentally determined reactions become evident above 3 GPa.

INTRODUCTION

Two factors have recently led to a renewed interest in the behavior of minerals at very high pressures. First, the ready availability of experimental apparatus capable of achieving pressures in the range of 20 GPa has led to an increase in the number and extent of experimental determinations of the stabilities of mineral phases, including hydrous silicates to these very high pressures (e.g., Pawley 1994; Schmidt and Poli 1994). Second, the increased attention of petrologists and geophysicists on the nature and behavior of the lithospheric slab as it descends into the mantle has raised several important questions concerning the amount and distribution of fluids at deep levels in subduction zones. Current thermodynamic models for hydrous and carbonate phases are not sufficiently complete to predict the temperatures and pressures of mineral decarbonation and dehydration reactions up to the pressures and temperatures prevailing in the deeper parts of subduction zones. Very basic data, such as the thermal expansivity and, more importantly, compressibility of common hydrous minerals likely to be important components in metamorphosed rocks in the descending slab, have not been measured, and simple linear extrapolations of molar volume, which are adequate for modeling crustal processes, are less accurate at the very high pressures of interest. Thus, we have selected four common mineral phases, which are believed to be likely hosts for transporting H_2O into the mantle in subduction zones, to measure their bulk moduli and extend our capability of calculating mineral assemblage stabilities at these high pressures and temperatures. The significance of three of these phases as potential hydrated silicates in subducted slabs [lawsonite (*Ccmm*), $CaAl_2Si_2O_7(OH)_2 \cdot H_2O$; zoisite (*Pnma*), $Ca_2Al_3Si_3O_{12}(OH)$; and clinozoisite (*Pnma*), $Ca_2Al_3Si_3O_{12}(OH)$] was discussed in the companion paper (Pawley et al. 1996).

In addition to these three phases, we also investigated the compressibility of epidote. Fe^{3+}-containing epidote ($P2_1/m$), $Ca_2Al_2FeSi_3O_{12}(OH)$, is common in rocks regionally metamorphosed under greenschist- and amphibolite-facies conditions. It also occurs in blueschists and eclogites crystallized in subduction-zone environments, and in some mafic igneous rocks. In experiments under possible subduction-zone P-T conditions, epidote of composition $Ca_2Al_{2.3}Fe_{0.7}Si_3O_{12}(OH)$ was found to be stable at pressures up to 3 GPa (Pawley and Holloway 1993). Its identification as monoclinic epidote, and not orthorhombic zoisite, was confirmed using Fourier-transform infrared spectroscopy.

SAMPLES AND EXPERIMENTAL TECHNIQUE

The samples of natural zoisite, clinozoisite, and synthetic lawsonite used in our measurements are the same as those described in the companion paper (Pawley et al. 1996). The sample of epidote is from a monomineralic vein in high-pressure albite-amphibolites from the Gross Venediger area in the central Höhe Tauern, Eastern Alps (Holland 1979; Holland and Ray 1985). It is very close to the end-member composition; chemical analyses, by electron microprobe, of the epidote and clinozoisite sam-

* Present address: Department of Earth Sciences, University of Manchester, Oxford Road, Manchester M13 9PL, U.K.

0003–004X/96/0304–0341$05.00

TABLE 1. Compositions of natural clinozoisite and epidote

	Clinozoisite		Epidote	
	wt%	Cations	wt%	Cations
SiO_2	39.58	2.989	38.01	3.013
TiO_2	0.0	0.0	0.04	0.002
Al_2O_3	33.65	2.996	21.41	2.001
Cr_2O_3	0.0	0.0	0.09	0.006
Fe_2O_3	0.34	0.019	16.12	0.961
FeO	0.0	0.0	0.26	0.017
MnO	0.0	0.0	0.06	0.004
MgO	0.0	0.0	0.0	0.000
CaO	24.70	2.000	23.48	1.996
Na_2O	0.0	0.0	0.0	0.0
K_2O	0.0	0.0	0.0	0.0

ples used in this study are given in Table 1. All the small amount of Fe in clinozoisite was assumed to be Fe^{3+} in the recalculation of the microprobe data; for the epidote sample, however, only a small proportion of Fe was assumed to be Fe^{2+}, and this quantity was calculated on the basis of eight cations per formula unit with 12.5 O atoms. Clean and clear individual crystals of zoisite, clinozoisite, and epidote were hand-picked from the natural samples, and they and a batch of the synthetic lawsonite were crushed and ground to a fine powder for X-ray diffraction experiments. Individual powder samples were mixed with powdered NaCl, which acted as an internal standard and pressure calibrant for the high-pressure measurements.

High-pressure powder diffraction was performed, in a manner identical to that used in the study of Redfern et al. (1993), on the wiggler station 9.7 of the SERC synchrotron radiation source at Daresbury, U.K. The powdered sample was loaded into a preindented, heat-treated Inconel gasket (200 mm hole) in a lever-arm diamond-anvil cell. A 4:1 nondried methanol-ethanol mixture was used as the pressure-transmitting medium. Measurements were made in energy-dispersive mode at room temperature between ambient pressure and 16 GPa. White radiation, collimated by a 150 μm pinhole, was diffracted at a fixed 2θ angle (accurately determined for each experiment from the diffraction pattern of NBS silicon powder) and further collimated using 500 mm long molybdenum receiving flats shimmed 100 μm apart. Spectra were collected between 5 and 120 keV using a lithium-drifted germanium detector with a resolution varying from 149 eV at 5.9 keV to 468 eV at 122 keV.

Pressure was calibrated with the use of the measured cell volume of the internal NaCl standard (determined from least-squares refinement of a minimum of three Bragg peaks) and the equation of state for NaCl given by Decker (1971). The estimated uncertainty in the pressure readings is $\pm 2\%$. Sample and NaCl diffraction peak positions were measured by Gaussian peak fitting of diffracted intensity. Values for unit-cell parameters were refined by a nonlinear least-squares method using the program UnitCell (Holland and Redfern in preparation), and from 7 to 15 peaks depending on sample and pressure. Typical diffraction patterns for the four samples under pressure loading are shown in Figure 1.

RESULTS

Values of cell parameters as a function of pressure are listed in Table 2 and plotted in Figures 2–5 as relative compressions. Uncertainties are shown only for relative volume compression for the sake of clarity in the figures. Values of the isothermal bulk modulus, K, and its pressure derivative, K', are commonly derived by fitting the pressure-volume data to the Birch-Murnaghan equation

$$P = \frac{3}{2}K\left[\left(\frac{V_0}{V}\right)^{\frac{7}{3}} - \left(\frac{V_0}{V}\right)^{\frac{5}{3}}\right]\left\{1 - \frac{3}{4}(4 - K')\left[\left(\frac{V_0}{V}\right)^{\frac{2}{3}} - 1\right]\right\}$$

or to the simpler Murnaghan equation

$$P = \frac{K}{K'}\left[\left(\frac{V_0}{V}\right)^{K'} - 1\right]$$

which may be conveniently rearranged into volume-explicit form,

$$\frac{V}{V_0} = \left[1 + \frac{K'}{K}P\right]^{-\frac{1}{K'}}.$$

We fitted our measured volume data with both the Birch-Murnaghan and Murnaghan equations and found that, over the pressure ranges of this study, both equations yield identical results within error. Rather than fit the data to the Birch-Murnaghan equation in the form above by minimizing residuals in pressure, we adapted a nonlinear least-squares routine to refine initial guesses for V_0, K_{298}, and K' by minimizing the residuals in volume (the measured parameter). The values for K_{298} and K' are often different when residuals in V rather than P are minimized, and the former is much the more useful because we wish to predict the volume from the pressure and not vice versa. Regression for three parameters, V_0, K_{298}, and K', is not warranted by the quality of the data especially because the parameters are very highly correlated (e.g., increasing K' reduces K_{298} and V_0). The scatter in our measured volumes is also too large to enable very precise values of K' to be determined, and attempts to obtain precise values for epidote and zoisite led to physically unrealistic (negative) values, the uncertainties of which were larger than the absolute values. Thus, we elected to set the pressure derivative K' to 4, a commonly accepted assumption that is based on the results of many measurements on silicate and oxide phases of geological interest and equivalent to reducing the Birch-Murnaghan equation to a simpler form by eliminating the final term (Anderson 1989; Liu and Bassett 1986). Nonlinear regression of the volume data can be found in Table 3.

DISCUSSION

The two mineral end-members of the monoclinic epidote solid-solution series, clinozoisite and epidote, show virtually identical compression behavior, with c being

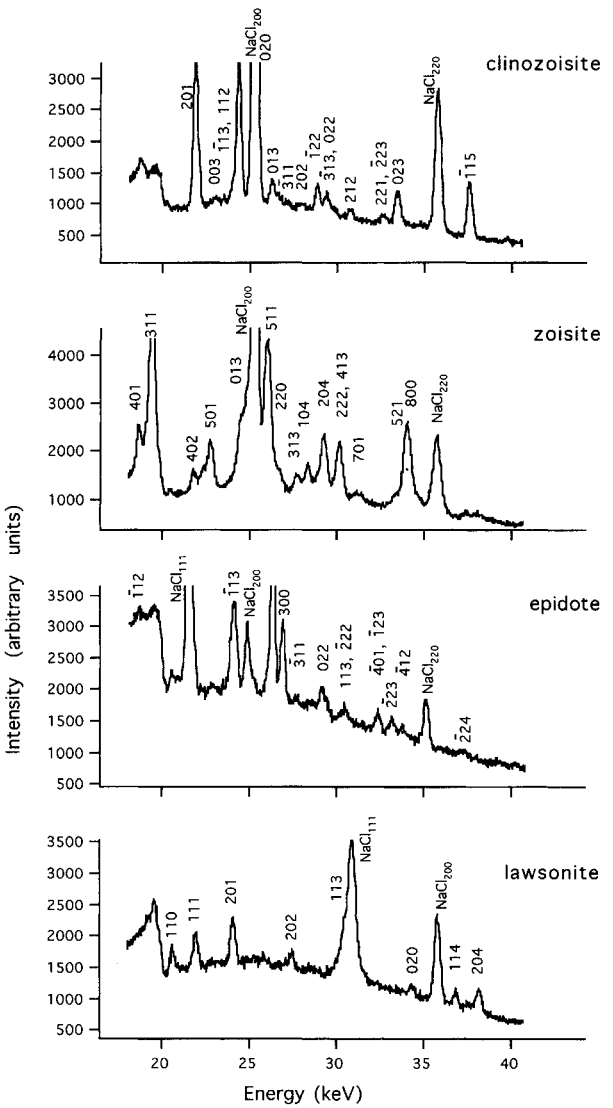

FIGURE 1. Energy-dispersive diffraction patterns of clinozoisite, zoisite, epidote, and lawsonite in the diamond-anvil cell at 1.5, 1.6, 0.4, and 0.7 GPa, respectively, displayed on a common energy scale. The step in the background (due mainly to Compton scattering in the diamonds) at ~20 keV is due to the absorption edge of diamond. The NaCl reflections are indicated, other peaks being indexed appropriately. The diffraction patterns of clinozoisite, zoisite, and epidote were collected with the detector at approximately 10.14° 2θ, and the diffraction pattern of lawsonite was collected with the detector fixed at 7.11° 2θ.

TABLE 2. High-pressure cell constants

P (GPa)	a (Å)	b (Å)	c (Å)	β (°)	V (Å³)
			Clinozoisite		
0.1	8.859(14)	5.588(6)	10.151(12)	115.46(10)	453.7(7)
1.31	8.845(16)	5.570(8)	10.103(15)	115.40(11)	449.6(8)
1.50	8.848(7)	5.579(7)	10.092(11)	115.39(7)	450.1(5)
2.13	8.826(12)	5.559(5)	10.098(13)	115.41(9)	447.5(6)
2.33	8.817(10)	5.568(6)	10.080(9)	115.41(7)	447.0(5)
3.17	8.814(11)	5.547(5)	10.058(12)	115.20(9)	444.9(6)
3.70	8.825(7)	5.535(4)	10.030(12)	115.30(7)	442.9(5)
4.58	8.790(16)	5.533(8)	10.027(27)	115.36(17)	439.9(10)
5.60	8.777(16)	5.531(7)	10.006(19)	115.24(12)	439.3(8)
6.69	8.779(13)	5.524(5)	9.966(22)	115.14(15)	437.5(8)
7.75	8.755(14)	5.504(5)	9.923(24)	115.18(16)	432.7(9)
8.20	8.757(31)	5.512(12)	9.918(75)	115.37(45)	432.6(28)
			Epidote		
0.0001	8.890(5)	5.641(3)	10.164(6)	115.55(7)	459.9(3)
0.05	8.894(7)	5.636(5)	10.162(9)	115.53(8)	459.6(5)
0.10	8.885(6)	5.640(6)	10.167(6)	115.53(6)	459.7(4)
0.41	8.896(7)	5.640(5)	10.165(1)	115.64(8)	459.8(4)
1.66	8.874(6)	5.623(5)	10.121(9)	115.62(6)	455.3(4)
2.95	8.865(4)	5.612(3)	10.109(5)	115.80(5)	452.8(2)
3.41	8.851(4)	5.608(3)	10.095(5)	115.80(6)	451.2(3)
4.24	8.836(5)	5.599(3)	10.060(6)	115.72(6)	448.4(3)
4.80	8.836(5)	5.596(4)	10.049(6)	115.83(6)	447.2(3)
5.21	8.827(8)	5.595(6)	10.030(8)	115.81(8)	445.9(6)
			Zoisite		
0.60	16.177(13)	5.554(7)	10.027(10)		901.0(12)
0.78	16.166(14)	5.552(7)	10.031(10)		900.3(12)
1.21	16.198(14)	5.549(6)	10.023(10)		900.8(12)
3.20	16.147(26)	5.539(14)	10.012(14)		895.4(20)
5.47	16.150(11)	5.494(3)	10.013(7)		888.4(6)
6.39	16.136(28)	5.503(9)	9.982(15)		886.3(19)
6.92	16.103(54)	5.487(19)	10.005(40)		884.0(37)
7.66	16.099(21)	5.504(7)	9.973(13)		883.7(15)
8.91	16.078(29)	5.476(12)	9.958(16)		876.8(21)
9.78	16.087(28)	5.473(9)	9.925(19)		873.8(20)
9.85	16.097(12)	5.459(5)	9.953(7)		874.5(9)
10.69	16.088(17)	5.462(10)	9.954(15)		874.6(16)
11.26	16.095(15)	5.431(10)	9.951(16)		869.8(17)
11.42	16.103(19)	5.421(8)	9.952(13)		868.7(13)
12.22	16.051(17)	5.444(13)	9.937(16)		868.4(12)
13.47	16.061(47)	5.390(16)	9.950(28)		861.2(30)
13.79	16.061(30)	5.418(30)	9.918(25)		863.1(42)
			Lawsonite		
0.07	8.782(5)	5.833(2)	13.097(9)		670.9(4)
0.81	8.772(10)	5.825(4)	13.083(15)		668.5(8)
1.51	8.752(7)	5.815(4)	13.064(17)		664.8(8)
2.31	8.742(7)	5.800(4)	13.059(16)		662.1(8)
2.46	8.747(6)	5.807(3)	13.063(9)		663.5(4)
3.68	8.718(11)	5.800(6)	13.019(16)		658.4(8)
4.38	8.713(7)	5.787(3)	13.010(9)		655.9(5)
4.87	8.697(11)	5.776(5)	13.015(16)		653.8(9)
5.72	8.705(17)	5.772(8)	13.016(25)		654.0(14)
6.66	8.683(21)	5.763(8)	12.993(31)		650.3(17)
7.64	8.667(19)	5.754(9)	12.983(27)		647.4(16)
8.75	8.649(25)	5.746(12)	12.948(37)		643.4(21)
9.97	8.626(23)	5.729(11)	12.967(34)		640.8(19)
10.30	8.614(44)	5.740(14)	12.954(46)		640.4(30)
10.84	8.609(47)	5.734(23)	12.956(79)		639.5(44)
11.21	8.615(20)	5.719(10)	12.914(29)		636.3(17)
11.40	8.625(31)	5.730(15)	12.958(54)		640.3(29)
12.05	8.613(44)	5.704(21)	12.930(75)		635.2(42)

most compressible and b and a being less affected. The orthorhombic polymorph, zoisite, is rather different in its compression from the two monoclinic members in that its b axis is most compressible, with a and c much less affected. Lawsonite compression mainly results in shortening of the a and b axes, with less pronounced shortening of the c axis. Although zoisite has a smaller volume at room pressure, the larger compressibility of clinozoisite means that the monoclinic phase becomes the denser of the two above ~2 GPa; from the thermal expansion measurements [companion paper (Pawley et al. 1996)] it was concluded that clinozoisite also becomes denser than zoisite above ~300 °C at room pressure. The large difference in bulk modulus between zoisite and clinozoisite is noteworthy because it is somewhat unexpected. Our

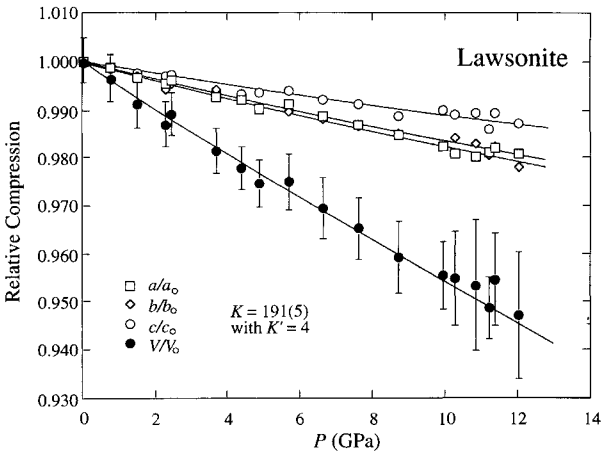

FIGURE 2. Relative compression of lawsonite. Variation of cell parameters, normalized to values at 1 bar, as a function of pressure. The curve for volume is a least-squares fit, giving K_{298} = 191 ± 5 GPa (Murnaghan EOS); those for individual cell parameters are just guides for the eye. Error bars for V/V_0 are two standard deviations; error bars on individual axial ratios are larger than symbols.

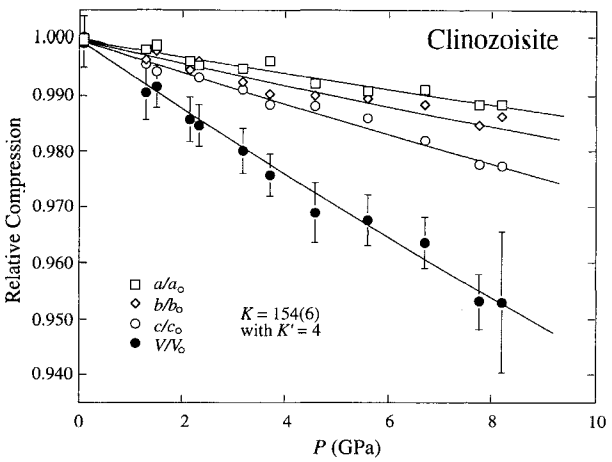

FIGURE 4. Relative compression of clinozoisite. Variation of cell parameters, normalized to values at 1 bar, as a function of pressure. The curve for volume is a least-squares fit, giving K_{298} = 154 ± 6 GPa (Murnaghan EOS); those for individual cell parameters are just guides for the eye. Error bars for V/V_0 are two standard deviations; error bars on individual axial ratios are larger than symbols.

data show that zoisite is far less compressible than clinozoisite. It would be convenient if we could offer a simple structural explanation for this difference, yet no other high-pressure study of these phases exists and the detailed structural responses to pressure must yet be identified. Comparing the Ca sites of zoisite and clinozoisite at ambient pressure and temperature, we observed that the Ca1 and Ca2 sites are significantly larger in the orthorhombic phase than in the monoclinic phase, and we would expect the Ca-O bond strength in zoisite to be weaker. Thus, the CaO_n polyhedra in zoisite might at first be expected to be more compressible, not less. Clearly the answer lies in some other aspect of the structure, possibly the influence of the AlO_6 octahedral chains and the silicate cross-linking. Furthermore, because the thermal expansion of zoisite is marginally greater than that of clinozoisite, increasing pressure in this phase cannot be thought of as volumetrically equivalent to decreasing temperature.

Zoisite is, therefore, the denser polymorph only close to ambient conditions. Under most metamorphic and all igneous conditions the denser phase is clinozoisite. These

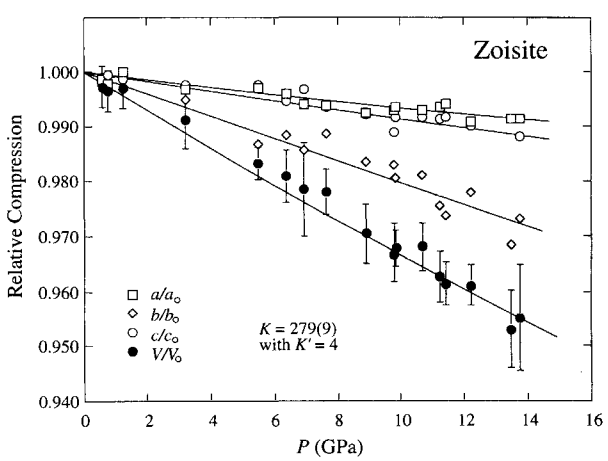

FIGURE 3. Relative compression of zoisite. Variation of cell parameters, normalized to values at 1 bar, as a function of pressure. The curve for volume is a least-squares fit, giving K_{298} = 279 ± 9 GPa (Murnaghan EOS); those for individual cell parameters are just guides for the eye. Error bars for V/V_0 are two standard deviations; error bars on individual axial ratios are larger than symbols.

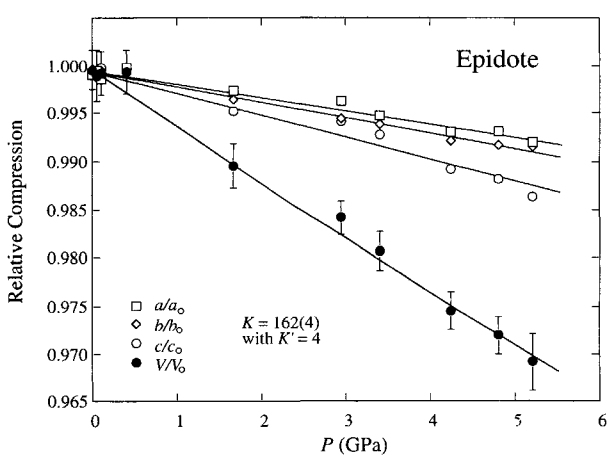

FIGURE 5. Relative compression of epidote. Variation of cell parameters, normalized to values at 1 bar, as a function of pressure. The curve for volume is a least-squares fit, giving K_{298} = 162 ± 4 GPa (Murnaghan EOS); those for individual cell parameters are just guides for the eye. Error bars for V/V_0 are two standard deviations; error bars on individual axial ratios are larger than symbols.

TABLE 3. Nonlinear regression of the volume data

	Murnaghan EOS		Birch-Murnaghan EOS	
	K_{298} (GPa)	V_0 (Å^3)	K_{298} (GPa)	V_0 (Å^3)
Lawsonite	191(5)	671.1(3)	191(6)	671.1(4)
Zoisite	279(9)	904.4(6)	267(9)	905.6(6)
Clinozoisite	154(6)	453.8(4)	154(7)	453.8(4)
Epidote	162(4)	460.3(2)	161(5)	460.3(3)

density relations should not be confused with the relative stability of the two polymorphs, which remains an unresolved problem and may require precise thermodynamic data to clarify given the sluggish kinetics of such transitions at low temperatures. However, although the arguments are beyond the scope of this paper and involve the relative heat capacities and entropies of the two polymorphs as well as natural Fe-Al partitioning, we believe that the transition has a steep positive dP/dT slope and occurs at temperatures near 350 °C, with zoisite as the stable phase on the high-temperature side (Holland in preparation). Thus, in the applications that follow, we calculate phase relations only at the elevated temperatures at which the orthorhombic form, zoisite, is stable.

To use both the compressibilities measured in this study and the thermal expansivities from the companion paper (Pawley et al. 1996) for thermodynamic calculations at high pressures and temperatures, we also need to estimate the temperature dependence of K, $\partial K/\partial T$. The bulk modulus K is approximately linear in T, and Anderson and Isaak (1993) showed that $\delta_T = -(1/\alpha K)(\partial K/\partial T)_P$. The quantity $\partial K/\partial T$ is approximately constant for each mineral, and the Anderson-Gruneisen parameter δ_T is a small positive number somewhat larger than K'. Taking $\partial K/\partial T$ to be proportional to $-\alpha K$ at 298 K, we found that the relationship $\partial K/\partial T = -7.0(\pm 1.0)\alpha_{298}K_{298}$ reproduces most of the known experimental data. In addition, if the thermal expansivities are represented by $\alpha = a_0 - 10a_0T^{1/2}$ as proposed in the companion paper (Pawley et al. 1996), then $\partial K/\partial T = -3a_0K_{298}$. In the thermodynamic calculations to follow we assume that $\partial K/\partial T$ is constant, and so $K_T = K_{298} - 3a_0K_{298}(T - 298)$.

The Murnaghan equation is quite adequate for calculating volumes to 20 GPa, and thus the pressure integral for the Gibbs energy may be written as

$$\int_0^P V\,dP = \frac{K_TV_T}{3}\left[\left(1 + \frac{4P}{K_T}\right)^{\frac{3}{4}} - 1\right]$$

where V_T is the ambient-pressure molar volume found from the expressions given in the companion paper (Pawley et al. 1996). The new formulation [above, and Pawley et al. (1996)] for thermal expansions and the Murnaghan equation for compressibilities are now used in a completely revised version of the internally consistent thermodynamic dataset and computer program THERMOCALC described by Holland and Powell (1990). This updated version also incorporates a large body of new experimental data as well as the CORK equations for gases at high pressure and temperature (Holland and Powell 1991). The basic thermodynamic data used are presented in Table 4, and the phase relations at high pressures are shown in Figures 6 and 7 for comparison with the recent experimental data of Pawley (1994), Skrok et al. (1994), and Schmidt and Poli (1994) as well as earlier experiments of Newton and Kennedy (1963) and Chatterjee et al. (1984) on lawsonite breakdown. Figure 6a shows the lawsonite breakdown reaction to zoisite + kyanite + quartz or coesite + H_2O and shows that agreement between calculations and experiment is excellent to 3 GPa but steadily worsens as pressure increases. This behavior was noted in the companion paper (Pawley et al. 1996) for diaspore breakdown to corundum + H_2O and therefore is probably a feature not specifically related to the thermodynamic properties of any of the solid phases in these reactions (none is involved in either reaction). The problem may be friction in the very-high-pressure

TABLE 4. Thermodynamic properties of selected phases in CASH

	H	sd(H)	S	V	a	b	c	d	a_0	K_{298}
Gr	−6640.81	3.39	0.256	12.535	0.6260	0	−5779.2	−4.0029	3.93	1680
Law	−4868.85	1.68	0.230	10.132	0.6878	0.1566	375.9	−7.1792	5.82	1910
Zo	−6897.65	2.82	0.296	13.575	0.5957	6.2297	−5921.3	−3.3947	6.77	2790
Ky	−2595.38	1.08	0.082	4.414	0.3039	−1.3390	−895.2	−2.9040	4.04	1590
Stv	−863.73	1.14	0.030	1.401	0.0681	0.6010	−1978.2	−0.0821	2.50	3100
Q	−910.75	0.45	0.0415	2.269	0.0979	−0.3350	−636.2	−0.7740	4.32	400
Bq	−908.41	0.45	0.04425	2.367	0.0979	−0.3350	−636.2	−0.7740	0.65	650
Coe	−907.64	0.45	0.0397	2.064	0.1087	−0.4387	0	−1.0725	1.94	1150
Tpz	−2905.44	1.42	0.1000	5.339	0.3877	−0.7120	−857.2	−3.7442	4.04	1315
Dia	−999.30	0.52	0.0353	1.776	0.1451	0.8709	584.4	−1.7411	7.97	2300
H_2O	−241.81	0.03	0.1888	0	0.0401	0.8656	487.5	−0.2512	0	0

Note: Mineral phases: Gr = grossular, Law = lawsonite, Zo = zoisite, Ky = kyanite, Stv = stishovite, Q = α quartz, Bq = β quartz, Coe = coesite, Tpz = hydroxy-topaz, Dia = diaspore, and H_2O = water. Symbols as in Holland and Powell (1990) except a_0 and K_{298}. Values for a_0 should be multiplied by 10^{-5}. The thermal expansions, α_T, and compressibilities, K_T, at high temperature are expressed as $\alpha_T = a_0 - 10a_0T^{-1/2}$ and $K_T = K_{298} - 3a_0K_{298}(T - 298)$, respectively (see text). The compressibility of diaspore is from Xu et al. (1994). The data for topaz were derived from the experiments of Wunder et al. (1993) using estimates of heat capacities and entropy [see Holland and Powell (1990) and Holland (1989) for methods]. Stishovite data were taken from Robie et al. (1979) and fitted to the experiments of Yagi and Akimoto (1976). High-pressure data for water were taken from the CORK equations (Holland and Powell 1991). Remaining data from Holland and Powell (1990), updated. Units are kilojoules, kelvins, and kilobars.

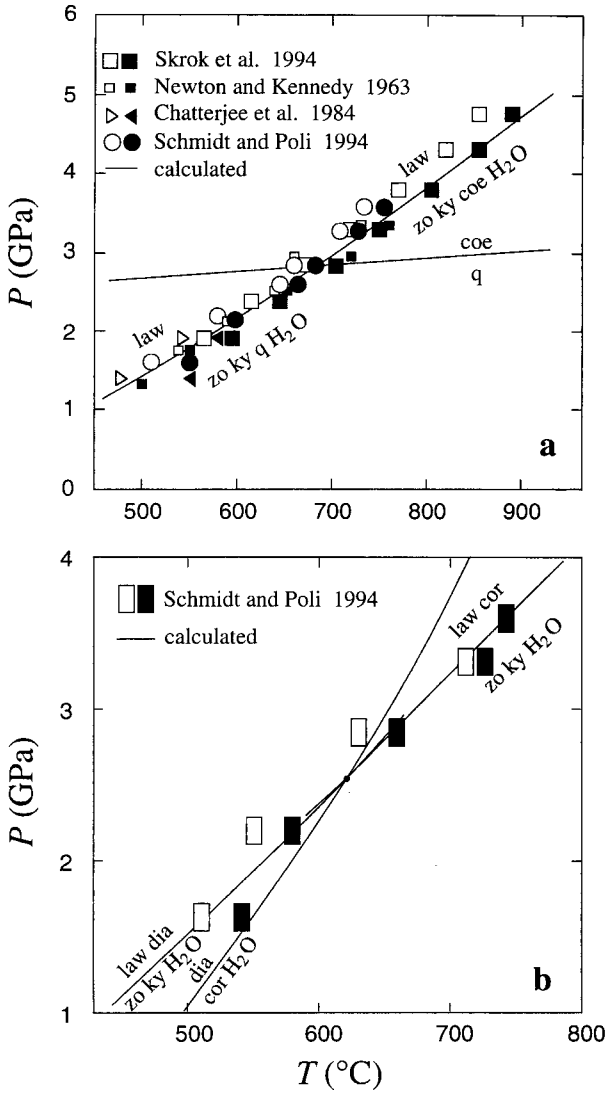

FIGURE 6. (a) Experimental brackets and calculated curves, using thermodynamic data from Table 4, for lawsonite breakdown. All pressures were corrected by −5% from the original experimental values to allow for a small friction effect in 0.5 in. piston-cylinder pressure cells. The coe = q curve was calculated from experiments of Bose and Ganguly (1995). (b) Experimental brackets and calculated curves for lawsonite + diaspore and lawsonite + corundum breakdown. H_2O data were calculated using the CORK (Holland and Powell 1991) equations and the volume data of Rice and Walsh (1957). Abbreviations: law = lawsonite, zo = zoisite, ky = kyanite, dia = diaspore, cor = corundum, coe = coesite, and q = quartz.

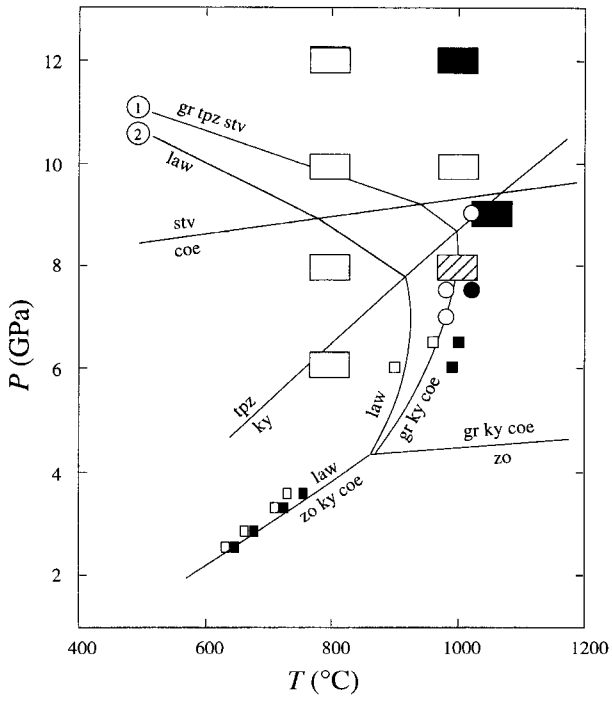

FIGURE 7. Experimental brackets and calculated curves for lawsonite breakdown at extreme pressures. Data used are described in the caption to Figure 6. Small squares = brackets of Schmidt and Poli (1994) on law = zo + ky + coe + H_2O; circles = brackets of Schmidt and Poli (1994) on law = gr + ky + coe + H_2O; large rectangles = experiments of Pawley (1994) (open = lawsonite growth, solid = gr + ky or tpz + stv or coe growth, hatch = law + gr + ky + coe). See text for discussion. Curve 1 is calculated using the high-pressure H_2O data of Brodholt and Wood (1993, 1994) and curve 2 using the data of Rice and Walsh (1957).

piston-cylinder experiments [changing the correction from −5 to −10% would bring good agreement as in the diaspore-corundum case mentioned in Pawley et al. (1996)] or it may be the thermodynamic properties of H_2O above 3 GPa. The calculated curves for the breakdown of lawsonite + diaspore are in quite good agreement (Fig. 6b) with the experiments of Schmidt and Poli (1994) at the comparatively low pressures of these experiments (<3.5 GPa). With these slight discrepancies appearing at higher pressures, we now consider the very-high-pressure experiments of Pawley (1994) and Schmidt and Poli (1994).

The calculated temperatures of dehydration reactions at very high pressures are rather sensitive to the volumes and fugacities assumed for water, and we show results (Fig. 7) for calculations based on extrapolations to 20 GPa using the Hugoniot-curve shock data of Rice and Walsh (1957) and the equation proposed by Brodholt and Wood (1993) from their molecular dynamics simulations. The Rice and Walsh measurements suggest smaller molar volumes at high pressures than the simulations of Brodholt and Wood, but the latter authors pointed out that (1) the shock temperatures are not well known, (2) their simulations are in good agreement with the *PVT* measurements of Burnham et al. (1969) at lower pressures, and (3) the simulations are in good agreement with the experimental fluid-inclusion volumes measured by Brodholt and Wood (1994). From Figure 7, the more reasonable agreement up to 8 GPa with the high-pressure phase-equilibrium experiments of Pawley (1994) and Schmidt and Poli (1994) also suggests that the Brodholt and Wood simulations may lead to the more reliable estimates of the very-high-pressure properties of water. We re-

fined the CORK equations of Holland and Powell (1991) so that a single expression can be used from 0 to 20 GPa, encompassing the low-pressure PVT data to 0.8 GPa and the high-pressure simulation results of Brodholt and Wood in the range 1–20 GPa. Only the virial-like terms in the CORK equation needed to be adjusted to fit all the data to within 0.6% average absolute deviation in volume, giving $V = V_{MRK} + c_1(P - P^0) + c_2(P - P^0)^{1/2} + c_3(P - P^0)^{1/4}$, with $c_1 = 2.1111 \times 10^{-3} - 5.20907 \times 10^{-7}T$, $c_2 = -9.17623 \times 10^{-2} + 1.12719 \times 10^{-5}T$, and $c_3 = 7.40395 \times 10^{-2}$, where $P^0 = 1.0$ kbar (0.1 GPa) and V_{MRK} is the molar volume from the Modified Redlich-Kwong equation calculated using Equations 3 and 6 of Holland and Powell (1991). All units for this EOS are in kilobars, kelvins, and kilojoules per mole.

Although the thermodynamic data for solids and water are in excellent agreement with the lawsonite breakdown reactions below 3 GPa shown in Figures 6a and 6b (as well as with several others, not shown, involving anorthite, pyrophyllite, and margarite), there are two serious discrepancies, which we cannot presently resolve, between calculated and experimental dehydration reactions at higher pressures. First, the calculated position of the reaction zoisite = grossular + kyanite + coesite + H_2O lies just above 4 GPa (Fig. 7), with small uncertainties (±0.1 GPa), in contrast with the experiments of Schmidt and Poli (1994), which locate it at ~6.7 GPa. There may have been some overstepping of pressure in the latter experiments, as the critical experiments defining the upper pressure limit were (1) unreversed, containing lawsonite and not grossular in the starting material [the lma experiments in Table 1 of Schmidt and Poli (1994)], and (2) were of very short duration (between 5 and 57 min). Additional experiments of longer duration, using reversal mixes, are needed to confirm the position of the zoisite breakdown reaction. However, it is unlikely that they would result in a depression of the reaction of more than a few hundred megapascals. The discrepancy between calculated and experimental reactions is thus very disconcerting because extremely large changes in the free energy of any one phase involved in the reaction would be required to bring the calculated and experimental pressures into agreement. By way of example, the Gibbs energy of zoisite would have to be reduced by over 20 kJ/mol to stabilize it from 4.2 to 6.7 GPa at 1000 °C. To obtain this from one of the first-order properties (S, V) would require changing the standard-state entropy by +15.7 J/(mol·K) or the molar volume by nearly −3 cm³/mol. Alternatively, the same effect could be produced by lowering the activity of pure zoisite by an order of magnitude from a value of 1.0 to ~0.1. Appealing to one of the second-order parameters, such as heat capacity, thermal expansion, or compressibility, would require totally unbelievable and unrealistic changes in these properties. Because of the stoichiometry of the reaction, even more drastic changes would be required of the Gibbs energies of H_2O (+60 kJ) or grossular (+30 kJ) to force the change in calculated pressure from 4.2 to 6.7 GPa. We do not believe that a case can seriously be made for any such extreme alterations in the thermodynamic properties of zoisite, grossular, kyanite, coesite, or H_2O because the many equilibria in which they are involved in the range 300–1400 °C and 0–3 GPa are consistent with, and impose extremely tight constraints upon, their thermodynamic properties.

The second major discrepancy between calculated and experimental reactions concerns the breakdown of lawsonite at extreme pressures (Fig. 7). At pressures up to 8 GPa there is reasonable agreement between the calculated position of the reaction lawsonite = grossular + kyanite + coesite + H_2O and the experimental results of Pawley (1994) and Schmidt and Poli (1994). However, although the experimental results suggest that the slope of the lawsonite breakdown reaction decreases gradually above 9 GPa, the calculations suggest a much sharper backbend. At present we can offer no solution to this dilemma, except to note the strongest remaining possibilities: (1) the properties of H_2O might change in hitherto unexpected ways at very high pressures, (2) the H_2O content of hydrous phases such as zoisite or lawsonite might change dramatically at high pressures, or (3) possible experimental problems, in the use of multi-anvil devices that require further investigation. Nevertheless, apart from the case of the very-high-pressure experiments, the thermodynamic calculations based on our new thermal expansions and compressibilities are in good mutual agreement with experimental observations.

Acknowledgments

A.R.P. wishes to acknowledge the support of NERC grant GR3/8362. We are grateful for the assistance of S.M. Clark and C.C. Tang at Daresbury Laboratory in making available their high-pressure facilities. Work at Daresbury Synchrotron Source was supported by the EPSRC in the form of minor grant 24/73.

References cited

Anderson, D.L. (1989) Theory of the Earth, 366 p. Blackwell Scientific, Oxford, U.K.

Anderson, O.L., and Isaak, D.G. (1993) Accuracy in measurements and the temperature and volume dependence of thermoelastic parameters. Pure and Applied Geophysics, 141, 327–339.

Bose, K., and Ganguly, J. (1995) Quartz-coesite transition revisited: Reversed experimental determination at 500–1200 °C and retrieved thermochemical properties. American Mineralogist, 80, 231–238.

Brodholt, J.P., and Wood, B.J. (1993) Simulations of the structure and thermodynamic properties of water at high pressures and temperatures. Journal of Geophysical Research, 98(B1), 519–536.

——— (1994) Measurements of the PVT properties of water to 25 kbars and 1600 °C from synthetic fluid inclusions in corundum. Geochimica et Cosmochimica Acta, 58, 2143–2148.

Burnham, C.W., Holloway, J.R., and Davis, N.F. (1969) Thermodynamic properties of water to 1000 °C and 10000 bars. Geological Society of America Special Paper 132, 96 p.

Chatterjee, N.D., Johannes, W., and Leistner, H. (1984) The system CaO-Al_2O_3-SiO_2-H_2O: New phase equilibria data, some calculated phase relations, and their petrological applications. Contributions to Mineralogy and Petrology, 88, 1–13.

Decker, D.L. (1971) High-pressure equation of state for NaCl, KCl, and CsCl. Journal of Applied Physics, 42, 3239–3244.

Holland, T.J.B. (1979) High water activities in the generation of high pressure kyanite eclogites of the Tauern Window, Austria. Journal of Geology, 87, 1–27.

——— (1989) Dependence of entropy on volume for silicate and oxide minerals: A review and a predictive model. American Mineralogist, 74, 5–13.

Holland, T.J.B., and Ray, N.J. (1985) Glaucophane and pyroxene breakdown reactions in the Pennine units of the eastern Alps. Journal of Metamorphic Geology, 3, 417–438.

Holland, T.J.B., and Powell, R. (1990) An enlarged and updated internally consistent thermodynamic dataset with uncertainties and correlations: The system K_2O-Na_2O-CaO-MgO-MnO-FeO-Fe_2O_3-Al_2O_3-TiO_2-SiO_2-C-H_2-O_2. Journal of Metamorphic Geology, 8, 89–124.

——— (1991) A Compensated-Redlich-Kwong (CORK) equation for volumes and fugacities of CO_2 and H_2O in the range 1 bar to 50 kbar and 100–1600 °C. Contributions to Mineralogy and Petrology, 109, 265–273.

Liu, L.G., and Bassett, W.A. (1986) Elements, oxides, and silicates, 250 p. Oxford University Press, Oxford.

Newton, R.C., and Kennedy, G.C. (1963) Some equilibrium reactions on the join $CaAl_2Si_2O_8$-H_2O. Journal of Geophysical Research, 68, 2967–2983.

Pawley, A.R. (1994) The pressure and temperature stability limits of lawsonite: Implications for H_2O recycling in subduction zones. Contributions to Mineralogy and Petrology, 118, 99–108.

Pawley, A.R., and Holloway, J.R. (1993) Water sources for subduction zone volcanism: New experimental constraints. Science, 260, 664–667.

Pawley, A.R., Redfern, S.A.T., and Holland, T.J.B. (1996) Volume behavior of hydrous minerals at high pressure and temperature: I. Thermal expansion of lawsonite, zoisite, clinozoisite, and diaspore. American Mineralogist, 81, 335–340.

Redfern, S.A.T., Wood, B.J., and Henderson, C.M.B. (1993) Static compressibility of magnesite to 20 GPa: Implications for $MgCO_3$ in the lower mantle. Geophysical Research Letters, 20, 2099–2102.

Rice, M.H., and Walsh, J.M. (1957) Equation of state of water to 250 kilobars. Journal of Chemical Physics, 26, 824–830.

Robie, R.A., Hemingway, B.S., and Fisher, J.R. (1979) Thermodynamic properties of minerals and related substances at 298.15 K and 1 bar (105 Pascals) pressure and at higher temperatures. U.S. Geological Survey Bulletin, 1452, 456 p.

Schmidt, M.W., and Poli, S. (1994) The stability of lawsonite and zoisite at high pressures: Experiments in CASH to 92 kbar and implications for the presence of hydrous phases in subducted lithosphere. Earth and Planetary Science Letters, 124, 105–118.

Skrok, V., Grevel, K.D., and Schreyer, W. (1994) Die Stabilität von Lawsonit, $CaAl_2[Si_2O_7](OH)_2 \cdot H_2O$, bei Drücken bis zu 50 kbar. European Journal of Mineralogy, 6, Beiheft no. 1, 270.

Wunder, B., Rubie, D.C., Ross, C.R., II, Medenbach, O., Seifert, F., and Schreyer, W. (1993) Synthesis, stability, and properties of $Al_2SiO_4(OH)_2$: A fully hydrated analogue of topaz. American Mineralogist, 78, 285–297.

Xu, J., Hu, J., Ming, L., Huang, E., and Xie, H. (1994) The compression of diaspore, AlO(OH) at room temperature up to 27 GPa. Geophysical Research Letters, 21, 161–164.

Yagi, T., and Akimoto, S. (1976) Direct determination of coesite-stishovite transition by in-situ X-ray measurements. Tectonophysics, 35, 259–270.

Manuscript received March 29, 1995
Manuscript accepted November 21, 1995